Tellus (2001), 53A, 629–641
Printed in UK. All rights reserved

TELLUS
ISSN 0280–6495

Freshwater forcing as a booster of thermohaline circulation

By JOHAN NILSSON[1]* and GÖSTA WALIN[2], [1]*Department of Meteorology, Stockholm University, Sweden;* [2]*Department of Oceanography, Göteborg University, Sweden*

(Manuscript received 1 November 2000; in final form 27 April 2001)

ABSTRACT

Making use of a simple two-layer model, we analyze the impact of freshwater forcing on the thermohaline circulation. We consider the forward-type circulation dominated by thermal forcing, implying that the freshwater forcing acts to reduce the density contrast associated with the equator-to-pole temperature contrast (prescribed in the model). The system is described by two variables: the depth of the upper layer (H) and the density contrast between the upper and lower layer ($\Delta\rho$), which decreases with salinity contrast. The rate of poleward flow of light surface water and the diapycnal flow (i.e., upwelling) driven by widespread small-scale mixing are both modeled in terms of H and $\Delta\rho$. Steady states of thermohaline circulation are found when these two flows are equal. The representation of the diapycnal flow (M_D) is instrumental for the dynamics of the system. We present equally plausible examples of a physically based representation of M_D for which the thermohaline circulation either decreases or increases with density contrast. In the latter case, contrary to the traditional wisdom, the freshwater forcing amplifies the circulation and there exists a thermally dominated equilibrium for arbitrary intensity of freshwater forcing. Here, Stommel's famous feedback between circulation and salinity contrast is changed from a positive to a negative feedback. The interaction of such a freshwater boosted thermohaline circulation with the climate system is fundamentally different from what is commonly assumed, an issue which is briefly addressed.

1. Introduction

1.1. Background

Conceptually, the thermohaline circulation can be divided in four branches. In the first branch, water is moving poleward in the upper ocean. The second branch involves descent into the deep ocean in high latitude convective regions. Equatorward motion in the deep ocean comprises the third branch. Upward motion through the stratification in low latitudes closes the circuit.

None of these branches has trivial dynamics, but the deep water formation has commonly been emphasized as the rate-limiting branch. It is easy to understand that a large transient input of freshwater in high latitudes might create a stable stratification, and thereby shut down the deep water formation (e.g., Rooth, 1982; Bryan, 1986; Tziperman, 2000). However, already Sandström (1908) put forward the argument that the strength of the thermohaline circulation (the Gulfstream in his terminology) is determined by the rate at which heat is transported downward in the upwelling branch. More recently, the rate-limiting role of deep water formation has been questioned by, for instance, Munk and Wunsch (1998), Marotzke and Scott (1999), and Huang (1999). Basically, they argue that the strength of the thermohaline circulation is related to the diapycnal mixing in the upwelling branch. The physical argument is essentially that the high-latitude convection releases potential energy from an unstable strati-

* Corresponding author address: Department of Meteorology, Stockholm University, 106 91 Stockholm, Sweden.
e-mail: nilsson@misu.su.se

fication. As long as the surface water is loosing buoyancy, convection is bound to take place. In the upwelling branch, on the other hand, energy has to be supplied to allow water to rise through the stable stratification.

If the upwelling branch is the rate-limiting factor of the thermohaline circulation it is conceivable that the circulation may be sensitive to the density contrast. Basic physics suggests that the diapycnal flow (i.e., the upwelling), sustained by small-scale vertical mixing, should decrease with increasing vertical density contrast. In the ocean, the vertical density contrast in low latitudes is basically the same as the equator-to-pole density contrast that drives the poleward flow in the surface layer. Thus, an increased oceanic density contrast should amplify the poleward surface flow but reduce the diapycnal flow. The final outcome, increased or decreased circulation, will depend on the physics that connects these two flows to the large-scale density structure.

Model studies indicate that the response of the thermohaline circulation to changes in density contrast is sensitive to the physical representation of the small-scale diapycnal mixing. For instance, Walin (1990) presents an idealized two-layer model that yields a thermohaline circulation that decreases with increasing density difference. Further, Lyle (1997) and Huang (1999) report ocean models of varying complexity which also produce a circulation that decreases with increasing density difference. The common feature of these three models is the representation of the vertical mixing, which is based on an assumption that the mixing energy is fixed irrespective of changes in the stratification. These models may be contrasted with models that represent the vertical mixing in terms of a constant diffusivity. It is well established that the thermohaline circulation increases with density difference in models using a fixed vertical diffusivity (e.g., Bryan, 1987; Zhang et al., 1999; Park and Bryan, 2000).

The present understanding of the diapycnal mixing in the ocean is not accurate enough to determine how these processes will respond to large changes in the stratification, for instance, associated with a glacial cycle. Therefore, the response of the thermohaline circulation to changes in the density difference may still be viewed as a challenging question.

1.2. Atmospheric thermally direct circulations

The possibility that the thermohaline circulation may be controlled by mixing in the upwelling branch and furthermore may decrease with increasing density contrast is far from an established view in oceanography. Therefore, it is instructive to consider an example from atmospheric dynamics, where it is well established that thermally direct* circulations are generally limited by processes in the non-convective descending branch of circulation (e.g., Emanuel et al., 1994; Pierrehumbert, 1995; Nilsson and Emanuel, 1999), corresponding to the upwelling branch of the thermohaline circulation. For instance, the intensity of the Hadley circulation is largely controlled in the descending branch. Similar to the thermohaline circulation (where the high latitude convection is highly localized), deep convection occurs only in a small fractional area of the Hadley cell. In the bulk of the domain, the air descends slowly in a cloud free stably stratified environment. Here, the leading order thermodynamic balance is

$$w\frac{\partial\theta}{\partial z} = Q, \tag{1}$$

where w is the vertical velocity, θ is the potential temperature, and Q is the heating rate per unit mass. In the tropics, the temperature stratification in the free atmosphere is essentially fixed at the moist adiabatic lapse rate (Emanuel et al., 1994). In the descending branch of the circulation, Q is set by the radiative cooling in cloud free skies, which is roughly constant (Emanuel et al., 1994; Pierrehumbert, 1995). As a result, the vertical motion in the descending branch is limited by the radiative cooling. In the ascending branch, on the other hand, latent heating in deep convective clouds can adjust to balance the adiabatic cooling of rising air.

1.3. Scope of the present study

If the thermohaline circulation decreases with increasing density difference, it will respond to

* In atmospheric science, thermally direct refers to circulations, driven by horizontally varying heating, in which the rising/sinking branch is co-located with the maximum in heating/cooling; e.g., the Walker and Hadley circulations.

freshwater forcing in a way that is fundamentally different from what is conventionally assumed. This is a key theme of the present study. To analyze the impact of freshwater forcing on the thermohaline circulation, we use an idealized two-layer representation of the ocean consisting of a surface layer floating above a lower layer, which outcrops in high latitudes. Simple physically based representations of the poleward surface flow and the diapycnal mixing are presented and applied in the model. At the present level of description, all effects related to wind driven circulation are ignored. In its interpretation, the present two-layer model differs from the classical two-box model of Stommel (1961), but the two model concepts share certain mathematical properties. The literature on thermohaline box models is large and growing. A good review of the subject is given by Marotzke (1996). The investigations with simple thermohaline models most pertinent to this study are Walin (1990), Zhang et al. (1999) and Park (1999). We review some of their results at appropriate points in our presentation.

2. The model

The model is based on the classic scaling of thermohaline circulation, which is succinctly reviewed by Welander (1986). In addition to conservation of mass, heat, and salt, this framework involves:

(1) the thermal wind balance [see eq. (6)];
(2) the advective–diffusive balance [see eq. (9)].

In what follows, we will use these conservation laws and dynamical relations to derive a two-layer model of the thermohaline circulation.

2.1. Conservation equations

Following Walin (1990), we consider a two-layer ocean model in which the upper layer and the bottom layer are distinguished by the subscripts 1 and 2, respectively (see Fig. 1). To simplify matters, we consider the limiting case of infinitely fast thermal adjustment, which implies that the temperatures T_1 and T_2 are fixed. Further, we take the poleward extent of the surface layer to be fixed in space. Conservation of volume is

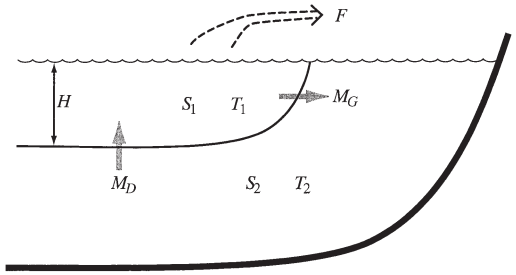

Fig. 1. An illustration of the model geometry. The subscripts 1 and 2 refer to the upper and the lower layer, respectively. Here, S is salinity, T is temperature, H is the upper layer depth, M_G is the poleward flow, M_D is the diapycnal flow, and F is the atmospheric freshwater transport.

given by

$$\frac{dV_1}{dt} = -M_G + M_D - F, \tag{2a}$$

$$\frac{dV_2}{dt} = +M_G - M_D + F, \tag{2b}$$

where F is the atmospheric freshwater transport, and M_G and M_D are the volume flows leaving and entering the upper layer, respectively. The depth, the area, and the volume of the upper layer are denoted H, A, and $V_1 = HA$, respectively. Salt conservation can be expressed as

$$\frac{dS_1V_1}{dt} = -S_1M_G + S_2M_D, \tag{2c}$$

$$\frac{dS_2V_2}{dt} = +S_1M_G - S_2M_D, \tag{2d}$$

where S denotes salinity.

By straightforward manipulations of eqs. (2a)–(2d), we obtain

$$V_1\frac{d\Delta S}{dt} = -\left[M_D + \frac{V_1}{V_2}M_G + \left(\frac{V_1}{V_2} - 1\right)F\right]\Delta S + F\left(1 + \frac{V_1}{V_2}\right)S_0, \tag{3}$$

where $\Delta S = S_1 - S_2$ and S_0 is the constant mean salinity of the system. We now make the following geophysically motivated approximations

$$V_1/V_2 \ll 1, \tag{4a}$$

$$F/M_G \ll 1, \quad F/M_D \ll 1, \tag{4b}$$

$$\Delta S/S_0 \ll 1. \tag{4c}$$

From eqs. (2a) and (3), we then obtain to the lowest order

$$A\frac{\mathrm{d}H}{\mathrm{d}t} = -M_{\mathrm{G}} + M_{\mathrm{D}}, \tag{5a}$$

$$AH\frac{\mathrm{d}\Delta S}{\mathrm{d}t} = -\Delta S M_{\mathrm{D}} + FS_0. \tag{5b}$$

This approximate system is described by the variables H and ΔS. We note that, in analogy with the Boussinesq approximation, F may be neglected in the mass balance (5a) despite its basic importance for the salinity balance (5b). In principle, the conditions (4a)–(4c) need to be checked *a posteriori*.

2.2. *The poleward flow, M_{G}*

The horizontal circulation is forced by gravity. Essentially, it is the tendency of light water to spread on top of denser water that drives the poleward flow in the upper ocean. Assuming that the circulation is in geostrophic and hydrostatic balance implies the thermal wind relation (e.g., Welander, 1986)

$$\frac{\partial u}{\partial z} = \frac{g}{f\rho_0}\frac{\partial \rho}{\partial y}, \tag{6}$$

where u is the zonal velocity, g is the acceleration of gravity, f is the Coriolis parameter, ρ_0 is a constant reference density, and y is the north–south coordinate. A scale analysis of eq. (6) (e.g., Welander, 1986; Park and Bryan, 2000) suggests that the poleward volume transport should obey

$$M_{\mathrm{G}} \sim \Delta\rho H^2, \tag{7}$$

where $\Delta\rho$ measures the density difference between the upper layer and the deep ocean as well as the equator-to-pole density difference. To illustrate the physics behind eq. (7), we may consider an upper layer of depth H, with a constant density anomaly $\Delta\rho$, which is bounded by a front where the deep water outcrops (see Fig. 1). By assuming that the deep water is at rest and integrating the thermal wind balance (twice vertically and once horizontally) across the front, we find that the volume transport (M) along the front is

$$M = \frac{g\Delta\rho H^2}{2f\rho_0}.$$

Primarily, eq. (7) is a measure of the zonal volume transport associated with the merdional density gradient. However, the ocean basins are longitudinally bounded by continents, which implies a basic correspondence between the strength of zonal and merdional transports. We may also view eq. (7) as representing the fraction of the zonal flow turned poleward when confronted with the eastern boundary of the basin. Accordingly, eq. (7) boils down to assuming that this fraction remains reasonably constant irrespective of changes in $\Delta\rho$ and H. Marotzke (1997) presents a slightly different line of argument showing that the east–west density difference in the thermocline should be proportional to the equator-to-pole density difference. This also serves to explain why the merdional transport may be estimated from the zonal thermal-wind relation. In addition to the basic physical motivation for eq. (7), it is corroborated by capturing reasonably the merdional flow in numerical models of thermohaline circulation (e.g., Bryan, 1987; Marotzke, 1997; Park and Bryan, 2000).

2.3. *The diapycnal flow, M_{D}*

It is considerably more difficult to represent the diapycnal flow, which is tied to the slow upwelling penetrating the stratified interior of the ocean. Presently, our knowledge of the small-scale mixing that drives the diapycnal flow is incomplete. To make progress, we assume that the diapycnal flow is controlled by the stratification in the upwelling region, characterized by the pycnocline depth-scale H and the density contrast $\Delta\rho$, and external factors, which for simplicity are taken to be constant. Specifically, we assume that the diapycnal flow is described by

$$M_{\mathrm{D}} \sim \Delta\rho^{-\zeta} H^{-\eta}, \tag{8}$$

where ζ and η may be varied in order to simulate different possible properties of the mixing and associated diapycnal flow. Intuitively, we expect that a deep pycnocline and/or a strong density contrast will reduce the diapycnal flow. Accordingly, we assume

$$\zeta \geqslant 0, \quad \eta \geqslant 0.$$

In what follows we will analyze the implications of different plausible choices of the pair (ζ, η). As a background, we will here discuss three assumptions concerning the small-scale mixing that lead

to different representations of M_D distinguished by the values of ζ and η. The common feature of these representations is that the diapycnal flow decreases with increasing density difference and upper-layer depth.

2.3.1. Constant vertical diffusivity, case A. Following Munk (1966), we assume that the stratification is governed by an advective–diffusive balance

$$w\frac{\partial\rho}{\partial z}=\frac{\partial}{\partial z}\left(\kappa\frac{\partial\rho}{\partial z}\right); \tag{9}$$

where w is the vertical velocity and κ is the vertical diffusivity. For a given stratification $\rho(z, H, \Delta\rho)$, we use eq. (9) to estimate the rate of diapycnal flow necessary to maintain the stratification.* For a constant vertical diffusivity, the diapycnal flow should obey (Welander, 1986)

$$M_D\approx\frac{A\kappa}{H}.$$

Since A as well as κ are assumed to be constant, we have

$$M_D\sim H^{-1}, \tag{10a}$$

i.e., $\zeta=0$, $\eta=1$.

If we, in this case, assume a vertically constant upwelling rate, eq. (9) yields the well known exponential density profile:

$$\rho(z, H, \Delta\rho)=\rho_0-\Delta\rho\exp(z/H),$$

where ρ_0 measures the deep water density.

2.3.2. Stability dependent diffusivity, case B. There is hardly observational support for a uniform vertical diffusivity in the ocean (e.g., Gargett, 1984; Polzin et al., 1997; Munk and Wunsch, 1998). In fact, Gargett (1984) presents observations indicating that the vertical diffusivity varies according to

$$\kappa=a_0N^{-1},\quad N=\left(-\frac{g}{\rho_0}\frac{\partial\rho}{\partial z}\right)^{1/2},$$

where a_0 is a constant and N is the buoyancy frequency. For this choice of diffusivity, a scale analysis of the advective–diffusive equation (9) yields

$$M_D\approx Aa_0\left(\frac{g\Delta\rho H}{\rho_0}\right)^{-1/2}.$$

This motivates the following diapycnal flow representation

$$M_D\sim\Delta\rho^{-1/2}H^{-1/2}, \tag{10b}$$

i.e., $\zeta=1/2$, $\eta=1/2$.

For the diffusivity proposed by Gargett (1984), it is easily verified that a stratification of the form

$$\rho(z, H, \Delta\rho)=\rho_0-\Delta\rho(1-z/H)^{-1},$$

represents a solution to eq. (9) with vertically uniform upwelling-rate as given by eq. (10b).

2.3.3. Constant mixing energy, case C. Walin (1990) makes use of an energy argument, originally put forward by Kato and Phillips (1969), to quantify M_D. Suppose that there is a fixed external energy supply (per unit area) to small-scale mixing. If $\mathscr{E}$ denotes the fraction of energy input that is used for work against the buoyancy force, then M_D should be of the form

$$M_D\approx\frac{A\mathscr{E}}{g\Delta\rho H},$$

suggesting the relation

$$M_D\sim\Delta\rho^{-1}H^{-1}, \tag{10c}$$

i.e., $\zeta=1$, $\eta=1$.

This formula relates the energy supply to small-scale mixing to the increase in potential energy in a two-layer system.

It is instructive to show that eq. (10c) may also be derived from the advective–diffusive balance (9) in a continuously stratified fluid, if it is the energy supply to small-scale mixing that is fixed rather than the diffusivity. In a Boussinesq fluid, the increase in potential energy (per unit area and time) due to vertical diffusion of density is given by (Munk and Wunsch, 1998)

$$\mathscr{E}=\rho_0\int\kappa N^2\,\mathrm{d}z, \tag{11}$$

where the integral runs over the depth of the ocean. In the simple case where κ is assumed to be uniform with depth, eq. (11) yields $\mathscr{E}=\kappa g\Delta\rho$. If $\mathscr{E}$ is constant, then the diffusivity has to vary

* Conceptually, it should emphasized that M_G, which forces the pycnocline upwards, is the advective component in the advective–diffusive balance. In a steady state, the upward advection equals the downward diapycnal velocity. Commonly, this balance is referred to as upwelling.

with vertical density difference according to

$\kappa = \mathscr{E}/(g\Delta\rho)$.

By substituting this expression for the diffusivity (which is assumed to be vertically uniform but varies horizontally with density difference between the bottom and surface of the ocean) into eq. (9) and performing a scale analysis, we recover eq. (10c).

2.4. Reference state and nondimensional equations

The density contrast entering the representations of M_G and M_D is assumed to be a linear function of the salinity contrast

$$\Delta\rho = \Delta\rho_0\left(1 - \frac{\rho_0\beta\Delta S}{\Delta\rho_0}\right), \tag{12}$$

where β is a constant haline-expansion coefficient and $\Delta\rho_0$ is the density contrast associated with the imposed temperature difference. Recall that the thermal adjustment is assumed to be instantaneous, which implies that $\Delta\rho_0$ is constant.

Suppose that we impose the density contrast $\Delta\rho_0$ and let the system evolve towards a steady state, which is attained when the depth is adjusted to some value H_0 that yields $M_G = M_D$, see eq. (5a). By denoting this flow by M_0, we define a reference state by

$$\Delta\rho = \Delta\rho_0, \quad H = H_0, \quad M_G = M_D = M_0. \tag{13}$$

Note that the freshwater forcing F and the salinity contrast ΔS are zero in the reference state.

We are not concerned here with the problem to find the relation between $\Delta\rho_0$, H_0, and M_0. Rather, the focus is to analyze the deviations from the reference state occurring when the freshwater forcing is introduced. For this purpose, we rewrite eqs. (7) and (8) as follows

$$M_G = M_0\left(\frac{\Delta\rho}{\Delta\rho_0}\right)\left(\frac{H}{H_0}\right)^2, \tag{14a}$$

$$M_D = M_0\left(\frac{\Delta\rho}{\Delta\rho_0}\right)^{-\zeta}\left(\frac{H}{H_0}\right)^{-\eta}, \tag{14b}$$

which together with the conservation relations (5a) and (5b) and the equation of state (12) specify our model.

We put the governing equations into nondimensional form using the scales of the reference state (13) and

$$t^* = (M_0/AH_0)t, \quad \Delta S^* = (\beta\rho_0/\Delta\rho_0)\Delta S, \tag{15}$$

where the asterisk denotes a nondimensional variable. The resulting nondimensional equations are (after dropping the asterisk)

$$\frac{dH}{dt} = -M_G + M_D, \tag{16a}$$

$$H\frac{d\Delta S}{dt} = -\Delta S M_D + R; \tag{16b}$$

where

$$M_G = \Delta\rho H^2, \tag{17a}$$

$$M_D = \Delta\rho^{-\zeta}H^{-\eta}, \tag{17b}$$

$$\Delta\rho = (1 - \Delta S). \tag{17c}$$

Note that $\Delta\rho$ is assumed to be positive as only the forward thermally dominated mode of circulation is considered. The system is governed by the nondimensional parameter:

$$R = \frac{F\beta S_0\rho_0}{M_0\Delta\rho_0}; \tag{18}$$

which measures the relative intensity of the freshwater forcing. It is instructive to estimate R based on the current state of the ocean. Considering a hemispheric basin, like the North Atlantic, we take $F \sim 10^5\ \mathrm{m^3\ s^{-1}}$ (see e.g., Wang et al., 1999, and references there), $M_0 \sim 10^7\ \mathrm{m^3\ s^{-1}}$ (strength of the thermohaline circulation), and $\beta S_0\rho_0/(\Delta\rho_0) \sim 20$; which suggests that $R \sim 0.2$.

3. Physical features of the model

The key theme is to analyze how the representation of the diapycnal flow affects the response of the model to freshwater forcing. Here, only the forward thermally dominated mode of circulation is considered.

3.1. Steady states

From the steady-state mass balance (16a) we obtain, using the expressions for M_G and M_D [eqs. (17a) and (17b)] the following relation between H and $\Delta\rho$:

$$\overline{H} = (\overline{\Delta\rho})^{(\lambda-1)/2} = (1 - \overline{\Delta S})^{(\lambda-1)/2}; \tag{19}$$

where the overbar is used to indicate an equilibrium state and, for notational convenience, we have introduced

$$\lambda = (\eta - 2\zeta)/(2 + \eta). \tag{20}$$

Inserting the relation (19) in the expression for M_G (or M_D), we obtain the steady state flow

$$\overline{M} = (\overline{\Delta\rho})^{\lambda} = (1 - \overline{\Delta S})^{\lambda}. \tag{21}$$

To close the problem we introduce eq. (21) into the salt balance (16b) to obtain an equation for ΔS

$$0 = -\overline{\Delta S}(1 - \overline{\Delta S})^{\lambda} + R. \tag{22}$$

We have assumed that ζ and η are positive, which implies that λ is always less than unity. Therefore, the upper-layer depth approaches infinity when the density contrast goes to zero; see eq. (19). Thus, a caveat to bear in mind is that the model may produce upper-layer depths that exceed the depth of the ocean.

Figure 2 shows how the circulation, salinity difference and the upper-layer depth, in equilibrium, vary with intensity of atmospheric freshwater transport. It is instructive to think that these graphs illustrate the evolution of the equilibria as the freshwater forcing is increased slowly enough

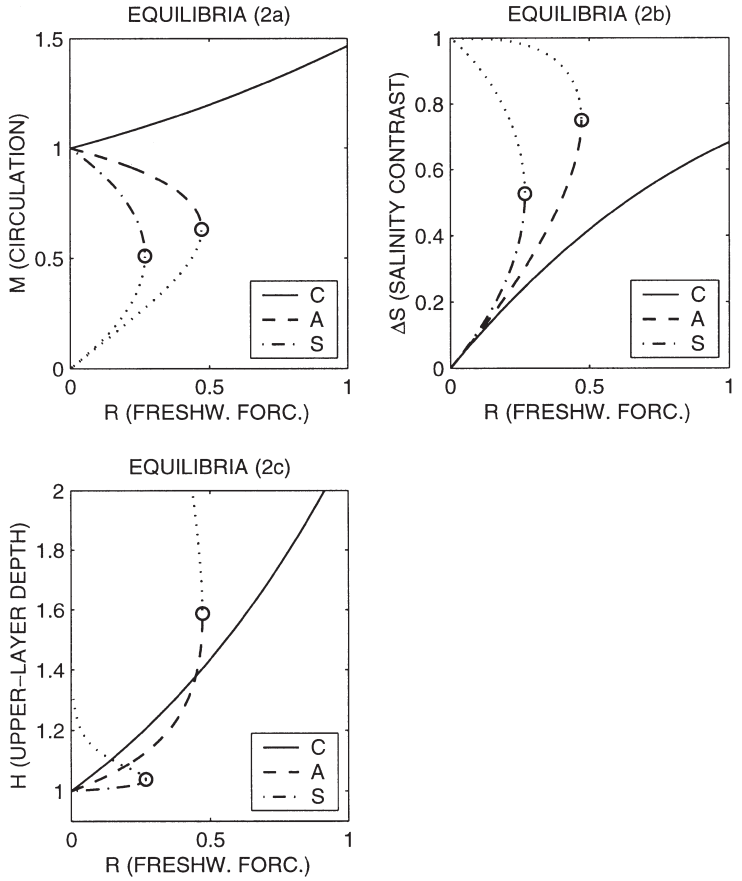

Fig. 2. Steady-state response of the model to freshwater forcing, delineated for three different representations of the diapycnal flow: model A ($\lambda = 1/3$), corresponding to constant diffusivity [see eq. (10a)]; model C ($\lambda = -1/3$), corresponding to constant mixing energy [see eq. (10c)]; and a hypothetical model S specified by $\lambda = 9/10$ [see eq. (20)]. The latter model is only selected for the purpose of comparison as it yields a system that operates similar to the classical model of Stommel (1961). The graphs portray two distinct regimes where the thermally-dominated forward circulation either increases (model C) or decreases (models A and S) with R. In the latter regime, the critical freshwater forcing (23) is marked with a circle and the unstable branches of steady states are illustrated by dotted lines. Panels a, b and c illustrate the response in circulation, salinity difference and pycnocline depth, respectively. Note that the three cases have identical equilibria in the absence of freshwater forcing: $\overline{\Delta S} = 0$, $\overline{H} = 1$ and $\overline{M} = 1$.

to keep the system in a quasi-steady state. The case $\lambda = 0$ (i.e., $\eta = 2\zeta$) discriminates between two fundamentally different modes of operation. It is easily verified that the representations A, B and C [eqs. (10a), (10b) and (10c)] yield $\lambda = 1/3$, $\lambda = -1/5$, and $\lambda = -1/3$, respectively. In Fig. 2 we have chosen to illustrate case A and C as well as a case with $\lambda = 0.9$. The latter case is selected not to portray any physically reasonable properties of the mixing, but rather to yield a system that operates similar to Stommel's classical model.

3.1.1. The freshwater boosted regime, $\lambda < 0$. We now assume that $\lambda < 0$, implying that $\eta < 2\zeta$. In view of the relation between M and $\Delta\rho$ given by eq. (21), we can directly see that the circulation will increase if the density difference decreases. As a result, the freshwater forcing, which acts to reduce $\Delta\rho$, will amplify the circulation and its attendant poleward heat transport as illustrated in Fig. 2a (for the case $\lambda = -1/3$). In passing, we note that introducing restoring boundary conditions on temperature in our model would weaken but not remove the increase in heat transport with freshwater forcing. We thus find that the well known feedback, pointed out by Stommel (1961), between circulation and freshwater forcing has changed sign and now acts to strengthen and stabilize the thermally dominated circulation. As a direct result, there exists a thermally dominated equilibrium for arbitrary amplitude of freshwater forcing. Furthermore, this state is always stable to small perturbations as shown in the appendix. Accordingly, the system cannot be forced out of the thermally dominated mode of operation even by very strong perturbations of the freshwater supply assuming that the perturbations are imposed slowly enough.

An increase in the freshwater forcing, as measured by the parameter R, will increase the depth of the upper layer but reduce the density contrast (Figs. 2b and c). This is true for all stable equilibrium solutions as long as $\lambda < 1$. In the freshwater boosted regime H and $\Delta\rho$ changes in such a manner that the quantity $\Delta\rho H^2$ increases despite the decreasing density contrast, which in view of eq. (17a) implies increasing flow.

3.1.2. The freshwater impeded regime, $\lambda > 0$. As shown directly by eq. (21), the circulation is now impeded by the decreased density contrast due to freshwater forcing. This depends on the parameterization of the diapycnal flow which does not allow the upper layer depth to increase sufficiently to compensate for the decreased density contrast. As a result the quantity $\Delta\rho H^2$ decreases with $\Delta\rho$ and so does the circulation.

In this regime, the steady-state features of the present model are similar, qualitatively, to those of the Stommel model with prescribed temperatures (e.g., Wallin, 1985; Marotzke, 1996). (In fact, when λ approaches unity the steady-state features of circulation and density difference are identical with the Stommel model; see below.) There exists a critical freshwater forcing, beyond which no thermally dominated equilibria are possible. To show this we may consider eq. (21). In the freshwater impeded regime where $\lambda > 0$, the left-hand side of this equation has a maximum value in the allowed range $0 < \Delta S < 1$, which determines a critical value of R, say R_c, as

$$R_c = \frac{1}{1+\lambda}\left(\frac{\lambda}{1+\lambda}\right)^{\lambda}. \tag{23}$$

When $R < R_c$, there exist two equilibria, but as in the Stommel model the equilibrium solution with weaker circulation is linearly unstable; see the appendix. The salinity contrast at $R = R_c$ is

$$\Delta S_c = \frac{1}{(1+\lambda)}. \tag{24}$$

This salinity contrast gives the lowest density difference at which a stable forward thermohaline equilibrium can be sustained.

It may be mentioned that Zhang et al. (1999) and Park (1999) present thermohaline models consisting of two vertically homogeneous boxes of fixed volumes, which have steady-state features that are mathematically similar to the present model with $\lambda = 1/3$ (i.e., case A in Section 2.3). They also use a relation between flow and density difference that is derived from the classical thermohaline scaling with constant vertical diffusivity (Welander, 1986), which yields a circulation that is proportional to $\Delta\rho^{1/3}$. Note, however, that this relation between flow and density difference follows from the adjustments in the pycnocline depth, which is a variable that is not represented in the box models of Zhang et al. (1999) and Park (1999).

3.2. *Feedbacks between circulation and freshwater forcing*

A striking consequence of a freshwater boosted circulation is that it changes Stommel's well known salinity feedback from a positive to a negative feedback. In the classical paradigm, the positive feedback between salinity anomalies and circulation depends on two basic features of the system (Stommel, 1961; Walin, 1985):

(i) The salinity contrast acts to reduce the density contrast which fuels the poleward flow.
(ii) The salinity contrast increases if the flow slows down.

The physics behind Stommel's feedback may be illustrated as follows. Suppose that the flow for some reason has temporarily slowed down. This slow state gives the freshwater forcing more time to operate and the salinity contrast is amplified. This will decrease the density contrast which acts to further slow down the circulation. Clearly, this mechanism represents a positive destabilizing feedback.

The fact that the strength of poleward flow also depends on the upper layer depth introduces an additional feedback in the scenario outlined above. It must be recognized that the key dynamical variables in the system (i.e., $\Delta\rho$ and H) are not independent. A perturbation in one will always be associated with a perturbation of the other. Suppose now that the enhanced salinity contrast and the connected weakening of the vertical density contrast are associated with an increased upper layer depth (which is the case in the present model as long as ζ and η are positive). This would act to increase the circulation. The final outcome, increased or decreased circulation, will then depend on which one of these feedback processes dominates.

As illustrated above the answer to this question depends on the dynamics in the upwelling branch, specifically on the features of the diapycnal mixing, which ultimately makes upwelling possible. When λ is negative in this model, item (i) above does not apply. Now, a salinity-related density reduction amplifies the circulation, hereby providing a negative feedback on perturbations of the salinity contrast. This negative feedback implies that the magnitude of ΔS stays modest even for large values of R as shown in Fig. 2b. This in turn means that the increased circulation to be expected in response to increased R, though positive, also remains modest. Essentially, the negative feedback implies that the system is relatively insensitive to variations in the freshwater forcing.

3.3. *Topographically constrained circulation*

Our model operates virtually as the Stommel model for $\lambda = 1$, which yields the most freshwater vulnerable circulation attainable with positive ζ- and η-values. However, η has to approach infinity (with ζ fixed and finite) to realize this limit. In this somewhat unphysical limit, the diapycnal flow is highly sensitive to the upper layer depth, which in effect becomes locked.

There is a geophysically relevant situation in which thermohaline circulation might operate, qualitatively, as in the infinite η-limit. This occurs when the deep water is formed in a semi-enclosed basin that is separated by a sill from the remainder of the ocean. If the upper layer equatorward of the sill is shallower than the sill depth, the depth variations can still have a stabilizing effect on the circulation in the freshwater boosted regime. When the upper layer extends below the sill, on the other hand, the sill presumably sets the depth of the poleward penetrating upper layer. As this occurs, we anticipate that the poleward transport across the sill is controlled chiefly by the density difference. Stigebrandt (1985) uses this line of argument to argue for a linear relation between density difference and transport in a study on thermohaline exchange between the North Atlantic and the northern North Atlantic over the Scotland–Greenland sill.

4. Discussion

We have analyzed the dynamics of a two-layer thermohaline model with a simple representation of the diapycnal flow, i.e., $M_D \sim \Delta\rho^{-\zeta} H^{-\eta}$ [see eq. (8)]. Depending on the relative influence of density difference and pycnocline depth on the diapycnal flow, we find two distinct regimes of thermohaline circulation:

(1) Freshwater boosted regime ($2\zeta > \eta$). Here, the circulation increases with decreasing density difference. As a result, the freshwater forcing amplifies the circulation and thereby the poleward

heat transport. Furthermore, Stommel's feedback between salinity- and circulation-anomalies has changed sign and acts to stabilize the system by keeping the salinity contrast down. This admits a linearly stable thermally dominated equilibrium for arbitrary amplitude of freshwater forcing.

Though it is remarkable that, in this regime, the circulation is in fact boosted by the freshwater supply, it should be remembered that since the feedback between circulation and salinity contrast is negative, the response to changes in the freshwater supply is generally small. Figure 2a (the case $\lambda = -1/3$) illustrates that even when R is increased to five times "normal" values (see end of Section 2.4) the circulation increases less than 50%. The diapycnal mixing representations denoted B (stability-dependent diffusivity) and C (constant mixing energy) in Section 2.3 yield models in this regime.

(2) Freshwater impeded regime ($2\zeta < \eta$). Here, the circulation increases with density difference. Accordingly, the freshwater forcing acts to weaken the circulation. The diapycnal representation A, corresponding to constant diffusivity, falls in this regime. Here no equilibria exist if the freshwater forcing exceeds a certain critical value as given by eq. (23). The main features of the system are qualitatively similar to those of the Stommel model with a prescribed temperature difference. The limit where η approaches infinity reproduces the classical Stommel model, which is the most freshwater sensitive case that can be represented with our description of diapycnal mixing.

We underline that it is possible to force a freshwater boosted thermohaline circulation out of the thermally dominated mode. The system is linearly stable, but a salinity perturbation large enough to reverse the equator-to-pole density gradient will still collapse the circulation. We have not attempted to model which state the thermohaline circulation attains after a breakdown. Walin (1990) identifies a stable, haline mode of circulation (low-latitude sinking) in his two-layer model, which is essentially identical to our model when the diapycnal representation C is used (i.e., $\zeta = 1$ and $\eta = 1$). He assumes that the reversed state has a structure similar to the forward state, but with the deep water outcropping on the equatorward side of the upper layer (see Fig. 1). This result suggests that a reversed freshwater-dominated circulation may also exist in the freshwater boosted regime. Thus, sufficiently strong perturbations may possibly cause a freshwater boosted system to transit between stable forward- and reversed-modes of circulation.

4.1. *Numerical model studies*

Contrary to the conventional wisdom, the present idealized model indicates that the thermohaline circulation may increase with decreasing density contrast, hereby allowing the freshwater forcing to amplify the circulation. However, to determine whether this is the case may be highly difficult from observations of the current state of the ocean. Palaeo-ocean data covering a glacial cycle, during which the intensity of the hydrological cycle changes substantially, would be more revealing. Numerical ocean circulation models provide an alternative method to analyze the response of the thermohaline circulation to changes in the equator-to-pole density difference.

Huang (1999) reports an interesting numerical study on thermally forced circulation. He considers a flat-bottomed hemispheric ocean model in the absence of freshwater- and wind-forcing. In the model, the sea surface temperature is relaxed towards a target temperature profile characterized by its north–south temperature difference. Huang describes two particularly interesting sets of simulations in which the equilibrium circulation is calculated for increasing north–south temperature difference. In the first set of simulations, a constant vertical diffusivity is used (our case A). Here, the circulation increases with density difference. In the second set, the vertical heat transport is calculated from a requirement of fixed energy for mixing. In this case, the response is the opposite: the circulation decreases with increasing density difference. As this case corresponds to our case C, the present idealized model appears to be consistent with the behavior of this particular numerical model. We anticipate that the circulation regime of Huang (1999) associated with fixed energy for mixing would be boosted if freshwater forcing is included.

In this context, it is relevant to mention the multi-box model of Lyle (1997), which also produces a thermally forced circulation that decreases with increasing density difference. The model of Lyle has one low- and one high-latitude region, which are horizontally homogeneous and verti-

cally subdivided in five boxes. There is no freshwater forcing, and the temperature is prescribed in the two surface boxes. The representation of the poleward flow is qualitatively similar to the one used here; see Section 2.2. The diapycnal flow is represented in terms of vertical diffusion. Lyle considers a constant diffusivity as well as a diffusivity that is inversely proportional to the density difference between bottom and surface in the low-latitude region. In the latter case, which corresponds to our case C, the circulation increases when the imposed surface-density difference is reduced.

Most numerical models with more realistic forcing and basin geometry appear to produce a thermohaline circulation that is impeded by freshwater forcing; see Rahmstorf (1999) and the references there. For instance, Rahmstorf (1995) and Tziperman (2000) report simulations with the GFDL model (in a coarse-resolution global configuration) in which the intensity of freshwater forcing is varied. Both studies find that the North Atlantic branch of thermohaline circulation decreases with freshwater forcing. It is interesting to note that these model simulations use a time independent vertical diffusivity that varies with depth, which is due to Bryan and Lewis (1979). Thus, based on our idealized model and the results reported by Huang (1999), one may be tempted to attribute the weakening of the thermohaline circulation in these models to the representation of diapycnal mixing (i.e., a stratification independent vertical diffusivity).

It is important to bear in mind, however, that other processes may prevent a freshwater amplification of the thermohaline circulation in the more complex models. One possibility is that the bulk of Atlantic deep water is formed in semi-enclosed basins, and that sills limit the flow as discussed in Section 3.3. Further, the wind driven component of circulation may exert a strong control on the pycnocline depth (see e.g., Pedlosky, 1996, chapter 7.1). This may curtail the stabilizing effect of pycnocline-depth adjustments, which is the key mechanism behind a freshwater boosted thermohaline circulation.

Moreover, it needs to be emphasized that the present model only considers a circulation that is confined in a single hemisphere. The real thermohaline circulation has a significant interhemispheric component, and furthermore it exchanges water between the Atlantic and the Pacific. It is beyond the scope of this work to address the influence of our diapycnal flow representation on an interhemispheric circulation. However, it is instructive to mention the numerical study of Wang et al. (1999). which illustrates that the freshwater forcing may amplify an interhemispheric circulation through an entirely different mechanism than the one studied here. Wang et al. (1999) consider an idealized representation of the Atlantic and Pacific basins, which are connected by a "Southern Ocean". Their model uses a fixed vertical diffusivity, and it is forced with a prescribed freshwater flux at the ocean surface that is symmetric with respect to the equator. Wang et al. (1999) find that the equilibrium merdional-overturning in the North Atlantic increases with freshwater forcing. Simultaneously, the rate of deep water formation in the southern hemisphere declines, which keeps the strength of the global thermohaline circulation nearly constant. The equatorially asymmetric thermohaline circulation is ultimately related to a pole-to-pole density difference in the deep ocean (e.g., Rooth, 1982; Scott et al., 1999; Klinger and Marotzke, 1999).

4.2. The thermohaline circulation and climate

We conclude with some speculative comments on climate related implications of a thermohaline circulation that is amplified by freshwater forcing. There are some indications that the deep ocean was warm during the Cretaceous period (see e.g., Brass et al., 1982; Lyle, 1997, and references therein), a period with a warm climate. A plausible interpretation of the warm deep water is that the hydrological cycle was intense enough to sustain a thermohaline circulation in the haline mode of operation, implying that warm, saline deep water was formed in low latitudes. However, if the ocean operates in the freshwater boosted regime, it is less likely that slow climatic changes in the hydrological cycle could terminate the forward mode of circulation. An alternative interpretation of the warm deep water, which is consistent with a forward thermally dominated circulation, can be conceived by noting that the pycnocline depth increases with freshwater forcing. Thus, an intense hydrological cycle may push the pycnocline deep into the ocean. This would not result in warm

bottom water but could radically change the hydrography at great depths.

Geochemical data suggest that the North Atlantic branch of the thermohaline circulation was weak and intermittent during the last ice age (e.g., Boyle and Keigwin, 1987). Further, studies using atmospheric circulation models indicate that the merdional atmospheric freshwater transport during the last glacial maximum was weaker than today (e.g., Lohmann and Lorenz, 2000). If we speculate that the change in thermohaline circulation was chiefly a response to the altered hydrological cycle, it is tempting to conclude that the circulation increases with freshwater forcing. Obviously, it is a challenging task to explore further the behavior of the thermohaline circulation in response to the great variations of the hydrological cycle that presumably occurred during glacial times. In particular the possibility that a weaker hydrological cycle may actually slow down the overturning of the ocean, as indicated by our analysis, is worthy of a serious consideration.

5. Acknowledgement

This work was supported by the Swedish Natural Science Council (NFR). The insightful and constructive criticism of two anonymous reviewers is highly appreciated. Further, we thank Drs. E. Tziperman and R. X. Huang for answering questions concerning their numerical simulations.

Appendix A

To analyze the linear stability of the equilibrium solutions, we write

$$H(t) = \overline{H} + H(t)', \quad \Delta S = \overline{\Delta S} + \Delta S(t)',$$

where the variables with over-bars and primes denote the equilibrium state and perturbations, respectively. Using this *ansatz* in eqs. (16a) and (16b) and keeping terms that are linear in the perturbed quantities, we get

$$\frac{\partial}{\partial t}\begin{pmatrix} H' \\ \Delta S' \end{pmatrix} = \begin{pmatrix} a & b \\ c & d \end{pmatrix}\begin{pmatrix} H' \\ \Delta S' \end{pmatrix}. \tag{A1}$$

The coefficients in the stability matrix are given by

$$a \equiv -\overline{H}(1-\overline{\Delta S})(2+\eta), \quad b \equiv \overline{H}^2(1+\zeta),$$

$$c \equiv \eta\overline{\Delta S}(1-\overline{\Delta S}), \quad d \equiv -\overline{H}[1+\overline{\Delta S}(\zeta-1)].$$

We seek solutions on the form $\exp(\sigma t)$ and (A1) determines the exponents:

$$\sigma_{1/2} = \frac{a+d}{2} \pm \left(\frac{(a+d)^2}{2} + bc - ad\right)^{1/2}. \tag{A2}$$

An equilibrium solution is stable if $a+d<0$ and $bc-ad<0$. Here, $\overline{\Delta S}<1$ and ζ and η are positive, which implies that $a<0$, $b>0$, $c>0$, and $d<0$. The condition $a+d<0$ is trivially satisfied in the present case. By using the definition of λ, the second stability condition can be expressed as

$$\overline{H}^2(1-\overline{\Delta S})(2+\eta)[\overline{\Delta S}(1+\lambda)-1]<0.$$

When $\lambda<0$, this condition is satisfied in the thermally dominated branch of equilibria where $\overline{\Delta S}<1$. When $\lambda>0$, on the other hand, the equilibria are linearly stable only if

$$\overline{\Delta S} < \frac{1}{(1+\lambda)} = \Delta S_c. \tag{A3}$$

Here, ΔS_c is the equilibrium salinity that results at the critical freshwater forcing R_c, see eqs. (23) and (24).

REFERENCES

Boyle, E. A. and Keigwin, L. 1987. North Atlantic thermohaline circulation during the past 20,000 years linked to high-latitude surface temperature. *Nature* **330**, 35–40.

Brass, G. W., Southam, J. R. and Peterson, W. H. 1982. Warm saline bottom water in the ancient ocean. *Nature* **296**, 620–623.

Bryan, F. 1986. High-latitude salinity effects and interhemispheric thermohaline circulations. *Nature* **323**, 301–323.

Bryan, F. 1987. Parameter sensitivity of primitive equation ocean general circulations models. *J. Phys. Oceanogr.* **17**, 970–985.

Bryan, K. and Lewis, L. J. 1979. A water mass model of the world ocean. *J. Geophys. Res.* **84**, 2503–2517.

Emanuel, K. A., Neelin, J. D. and Bretherton, C. S. 1994. On large-scale circulations in convecting atmospheres. *Q. J. R. Meteorol. Soc.* **120**, 1111–1143.

Gargett, A. E. 1984. Vertical eddy diffusivity in the ocean interior. *J. Mar. Res.* **42**, 359–393.

Huang, R. X. 1999. Mixing and energetics of the oceanic thermohaline circulation. *J. Phys. Oceanogr.* **29**, 727–746.

Kato, H. and Phillips, O. M. 1969. On the penetration of a turbulent layer into a stratified fluid. *J. Fluid Mech.* **37**, 643–655.

Klinger, B. A. and Marotzke, J. 1999. Behavior of double-hemisphere thermohaline flows in a single basin. *J. Phys. Oceanogr.* **29**, 382–399.

Lohmann, G. and Lorenz, S. 2000. On the hydrological cycle under paleoclimatic conditions as derived from AGCM simulations. *J. Geophys. Res.* **D13**, 17417–17436.

Lyle, M. 1997. Could early Cenozoic thermohaline circulation have warmed the poles. *Paleoceanography* **12**, 161–167.

Marotzke, J. 1996. Analysis of thermohaline feedbacks. In: *Decadal climate variability; dynamics and predictability* (eds D. L. T. Anderson and J. Willebrand), Vol. I 44, NATO ASI series, Springer-Verlag, 334–378.

Marotzke, J. 1997. Boundary mixing and the dynamics of three-dimensional thermohaline circulations. *J. Phys. Oceanogr.* **27**, 1713–1728.

Marotzke, J. and Scott, J. R. 1999. Convective mixing and the thermohaline circulation. *J. Phys. Oceanogr.* **29**, 2962–2970.

Munk, W. H. 1966. Abyssal recipes. *Deep-Sea Res.* **13**, 707–730.

Munk, W. H. and Wunsch, C. 1998. Abyssal recipes II: energetics of tidal and wind mixing. *Deep-Sea Res.* **I 45**, 1977–2010.

Nilsson, J. and Emanuel, K. A. 1999. Equilibrium atmospheres of a two-column radiative-convective model. *Q. J. R. Meteorol. Soc.* **125**, 2239–2264.

Park, Y.-G. 1999. The stability of thermohaline circulation in a two-box model. *J. Phys. Oceanogr.* **29**, 3101–3110.

Park, Y.-G. and Bryan, K. 2000. Comparison of thermally driven circulation from a depth-coordinate model and an isopycnal model. Part I: scaling-law sensitivity to vertical diffusivity. *J. Phys. Oceanogr.* **30**, 590–605.

Pedlosky, J. 1996. *Ocean circulation theory*. Springer-Verlag, first edition, 453 pp.

Pierrehumbert, R. T. 1995. Thermostats, radiator fins, and the local runaway greenhouse. *J. Atmos. Sci.* **52**, 1784–1806.

Polzin, K. L., Toole, J. M., Ledwell, J. R. and Schmitt, R. W. 1997. Spatial variability of turbulent mixing in the abyssal ocean. *Science* **276**, 93–96.

Rahmstorf, S. 1995. Bifurcations of the Atlantic thermohaline circulation in response to changes in the hydrological cycle. *Nature* **378**, 145–149.

Rahmstorf, S. 1999. Shifting seas in the greenhouse. *Nature* **399**, 523–524.

Rooth, C. 1982. Hydrology and ocean circulation. *Prog. Oceanogr.* **11**, 131–149.

Sandström, J. W. 1908. Dynamische versuche mit meerwasser. *Annalen der Hydrographie und Maritimen Meteorologie* **36**, 6–23.

Scott, J. R., Marotzke, J. and Stone, P. H. 1999. Interhemispheric thermohaline circulation in coupled box model. *J. Phys. Oceanogr.* **29**, 351–365.

Stigebrandt, A. 1985. On the hydrographic and ice conditions in the northern North Atlantic during different phases of a glaciation cycle. *Palaeogeogr., Palaeoclimatol., Palaeoecol.* **50**, 303–321.

Stommel, H. M. 1961. Thermohaline convection with two stable regimes of flow. *Tellus* **13**, 224–230.

Tziperman, E. 2000. Proximity of the present day thermohaline circulation to an instability threshold. *J. Phys. Oceanogr.* **30**, 90–104.

Walin, G. 1985. The thermohaline circulation and the control of ice ages. *Palaeogeogr., Palaeoclimatol., Palaeoecol.* **50**, 323–332.

Walin, G. 1990. On the possibility of a reversed thermohaline circulation. In: *Nordic perspectives on oceanography* (ed. P. Lundberg), Kungl. Vetenskaps- och Vitterhets-Samhället i Göteborg., 145–154. (Available from the author, Earth Science Center, Göteborg University, Box 460, 40530 Gothenburg, Sweden).

Wang, X., Stone, P. H. and Marotzke, J. 1999. Global thermohaline circulation. Part I: sensitivity to atmospheric moisture transport. *J. Climate* **12**, 71–82.

Welander, P. 1986. Thermohaline effects in the ocean circulation and related simple models. In: *Large-scale transport processes in the oceans and atmosphrere* (eds J. Willebrand and D. L. T. Anderson). D. Reidel, 163–200.

Zhang, J., Schmitt, R. W. and Huang, R. X. 1999. The relative influence of diapycnal mixing and hydrological forcing on the stability of thermohaline circulation. *J. Phys. Oceanogr.* **29**, 1096–1108.